

# Trilinear Higgs boson coupling variations for di-Higgs production with full NLO QCD predictions in Powheg

G. Heinrich<sup>1</sup>, S. Jones<sup>2</sup>, M. Kerner<sup>3</sup>, G. Luisoni<sup>1</sup> and L. Scyboz<sup>1</sup>

<sup>1</sup> Max-Planck-Institut für Physik, Föhringer Ring 6, 80805 München, Germany

<sup>2</sup> Theoretical Physics Department, CERN, Geneva, Switzerland

<sup>3</sup> Physik-Institut, Universität Zürich, Winterthurerstrasse 190, 8057 Zürich, Switzerland

E-mail: gudrun@mpp.mpg.de, s.jones@cern.ch, mkerner@physik.uzh.ch,  
luisonig@gmail.com, scyboz@mpp.mpg.de

**Abstract.** The couplings of the Higgs boson to other particles are increasingly well measured by the ATLAS and CMS experiments. The Higgs boson trilinear self-coupling however is still largely unconstrained, mainly due to the low cross-section for Higgs boson pair production. We present inclusive and differential results for the NLO QCD corrections to Higgs boson pair production with the full top-quark mass dependence, where the Higgs trilinear coupling is varied to non-SM values. The calculation of the two-loop virtual contributions has been performed numerically using CPUs and GPUs. The fixed-order calculation is supplemented by parton showering within the `Powheg-BOX-V2` event generator, and both `Pythia8` and `Herwig7` parton-shower algorithms are implemented in a preliminary study of shower effects.

## 1. Introduction

Impressive experimental constraints have been set on the Higgs boson couplings to vector bosons and heavy fermions [1, 2, 3, 4]. The Higgs potential, in contrast, leaves more room for New Physics. In particular, the Higgs boson trilinear self-coupling  $\lambda$  can be experimentally constrained by exclusion limits on Higgs boson pair production  $pp \rightarrow hh$  [5, 6]. Higher-order corrections to Higgs pair production were first calculated in the heavy top-quark mass limit (HTL)  $m_t \rightarrow \infty$ , where the top-quark degrees of freedom are integrated out [7, 8, 9, 10]. The NLO QCD corrections with the full top-quark mass dependence were only computed more recently [11, 12, 13]. They are based on numerical evaluations of the two-loop contribution to  $gg \rightarrow hh$ . For non-SM values of the Higgs couplings, results were computed at NLO QCD with the full top-quark mass dependence for a class of extensions of the SM in Ref. [14].

In the following, an implementation of the full NLO QCD corrections into the `Powheg-BOX-V2` event generator [15, 16, 17] is presented. In this framework, the Higgs trilinear self-coupling can be varied, as well as the top-Higgs Yukawa coupling. Total cross sections are computed for  $\sqrt{s} = 13, 14$  and 27 TeV at the (HE-)LHC. Differential results are shown for  $\sqrt{s} = 14$  TeV. The fixed-order calculation is then matched to both `Pythia8` [18] and `Herwig7` [19] parton showers. For a more detailed description, the reader is referred to Ref. [20].

## 2. Description of the calculation

The calculation is based on the setup presented in Ref. [21] for the case of the SM. The leading-order amplitude has been computed analytically. The real-emission contributions were

implemented using an interface [22] between the `Powheg-BOX` and `GoSAM` [23, 24], where the reduction of the one-loop amplitude has been performed with `Ninja` [25], using master integrals from `golem95C` [26, 27], `OneLOop` [28] and `VBFNLO` [29, 30]. The two-loop amplitude for the full virtual contribution was adapted from Refs. [11, 12], which used an extension of the `GoSAM` package to two loops [31]. There, the integral reduction was performed with `REDUZE2` [32], and the integrals were numerically evaluated with `SECDEC3` [33]. For a fast convergence, the integration was performed within a Quasi-Monte-Carlo implementation using a rank-1 shifted lattice rule [34, 35]. The integrals were computed with 16 dual NVIDIA TESLA K20XM GPUs. The top-quark and Higgs masses have been set to  $m_t = 173$  GeV and  $m_h = 125$  GeV. Thus, the integrals depend only on the two Mandelstam invariants  $\hat{s}$  and  $\hat{t}$ .

A grid for the two-loop amplitude was constructed in both variables using 5291 pre-sampled phase-space points. We split the amplitude in two contributions: diagrams containing the trilinear Higgs coupling are called *triangle-like*, and those that do not are called *box-like* (see Fig. 1 for two leading-order diagrams).

*Comment: it would be more instructive to show two-loop diagram examples*



**Figure 1.** Triangle-like (left) and box-like (right) diagrams contribute to the full amplitude. The former contain the Higgs self-coupling, while the latter do not.

At any order in QCD, the squared matrix-element can thus be written as a second-order polynomial in  $\lambda$ :

$$M_\lambda \equiv |\mathcal{M}_\lambda|^2 = \mathcal{M}_B^* \mathcal{M}_B + \lambda (\mathcal{M}_B^* \mathcal{M}_T + \mathcal{M}_T^* \mathcal{M}_B) + \lambda^2 \mathcal{M}_T^* \mathcal{M}_T. \quad (1)$$

The two-loop amplitude for an arbitrary value of  $\lambda$  can be reconstructed from the squared matrix-element computed for three different values of  $\lambda$ . In our case, we chose  $\kappa_\lambda = \lambda_{\text{BSM}}/\lambda_{\text{SM}} \in \{-1, 0, 1\}$ . A new grid is generated at runtime for the user-defined value of  $\lambda$ , where the amplitude for each pre-sampled phase-space point is calculated as:

$$M_\lambda = M_0 \cdot (1 - \lambda^2) + \frac{M_1}{2} \cdot (\lambda + \lambda^2) + \frac{M_{-1}}{2} \cdot (-\lambda + \lambda^2). \quad (2)$$

The grid produced for the two-loop amplitude is fed to an interpolation framework, which interfaces the result at *any* phase-space point  $M_\lambda(\hat{s}, \hat{t})$  to `Powheg`.

### 3. Total and differential cross-sections for variations of the trilinear coupling

The results given below are produced using the `PDF4LHC15_nlo_30_pdfas` sets [36, 37, 38, 39] interfaced to `Powheg` via `LHAPDF6` [40], with the corresponding value of  $\alpha_s$ . The top-quark mass is renormalised in the on-shell scheme and is set to  $m_t = 173$  GeV, as in the virtual amplitude. The mass of the Higgs boson is fixed to  $m_h = 125$  GeV, and the top-quark and Higgs widths are set to zero. Jets are clustered using the anti- $k_T$  algorithm [41] as implemented in `FastJet` [42, 43], with a jet distance parameter of  $R = 0.4$  and a minimum transverse momentum requirement of  $p_T = 20$  GeV. The central renormalisation and factorisation scales

are set to  $\mu_R = \mu_F = \mu_0 = m_{hh}/2$ . Scale uncertainties are estimated by 2-point variations  $\mu_R = \mu_F = c\mu_0$ , with  $c \in \{0.5, 2.0\}$ .

Total cross-sections for Higgs pair production at the (HE-)LHC are shown in Table 1, for centre-of-mass energies of  $\sqrt{s} = 13, 14$  and 27 TeV and different values of the Higgs self-coupling  $\kappa_\lambda = \lambda_{\text{BSM}}/\lambda_{\text{SM}}$ . They are accompanied by their relative scale uncertainties, which are of the order  $\mathcal{O}(10-20\%)$ . Notably, the  $K$ -factors at 14 TeV show a sizeable dependence on the trilinear coupling  $\kappa_\lambda$ . In the HTL at NLO QCD, Ref. [44] suggested a variation of the  $K$ -factors with  $\kappa_\lambda$  of the order  $\mathcal{O}(2-3\%)$ . In the full theory, the  $K$ -factors are found to vary between 1.56 and 2.15 for variations of the trilinear coupling  $-5 \leq \kappa_\lambda \leq 12$ , see Fig. 2.

$\lambda_{\text{BSM}}/\lambda_{\text{SM}}$	$\sigma_{\text{NLO}}@13\text{TeV}$ [fb]	$\sigma_{\text{NLO}}@14\text{TeV}$ [fb]	$\sigma_{\text{NLO}}@27\text{TeV}$ [fb]	K-factor@14TeV
-1	$116.71^{+16.4\%}_{-14.3\%}$	$136.91^{+16.4\%}_{-13.9\%}$	$504.9^{+14.1\%}_{-11.8\%}$	1.86
0	$62.51^{+15.8\%}_{-13.7\%}$	$73.64^{+15.4\%}_{-13.4\%}$	$275.29^{+13.2\%}_{-11.3\%}$	1.79
1	$27.84^{+11.6\%}_{-12.9\%}$	$32.88^{+13.5\%}_{-12.5\%}$	$127.7^{+11.5\%}_{-10.4\%}$	1.66
2	$12.42^{+13.1\%}_{-12.0\%}$	$14.75^{+12.0\%}_{-11.8\%}$	$59.10^{+10.2\%}_{-9.7\%}$	1.56
2.4	$11.65^{+13.9\%}_{-12.7\%}$	$13.79^{+13.5\%}_{-12.5\%}$	$53.67^{+11.4\%}_{-10.3\%}$	1.65
3	$16.28^{+16.2\%}_{-15.3\%}$	$19.07^{+17.1\%}_{-14.1\%}$	$69.84^{+14.6\%}_{-12.1\%}$	1.90
5	$81.74^{+20.0\%}_{-15.6\%}$	$95.22^{+19.7\%}_{-11.5\%}$	$330.61^{+17.4\%}_{-13.6\%}$	2.14

**Table 1.** Total cross-sections for Higgs boson pair production at NLO QCD at (HE-)LHC for centre-of-mass energies of  $\sqrt{s} = 13, 14$  and 27 TeV. The scale uncertainties are given in percent.

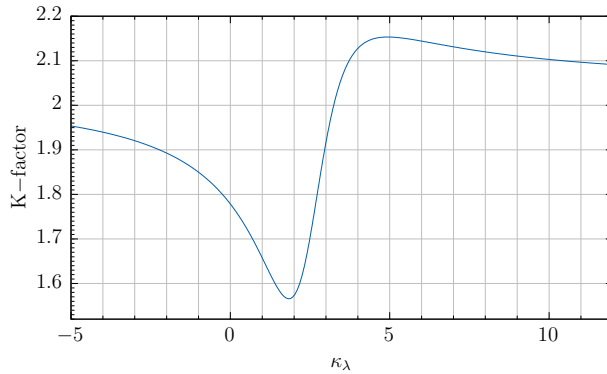


**Figure 2.** The dependence of the  $K$ -factor on the trilinear Higgs self-couplings  $\kappa_\lambda$  is given at  $\sqrt{s} = 14$  TeV in the full theory.

In Fig. 3, distributions of the invariant mass  $m_{hh}$  of the Higgs boson pair system are displayed for different values of  $\kappa_\lambda$ . They exhibit a characteristic dip around  $m_{hh} \sim 350$  GeV for values of the trilinear coupling around  $\kappa_\lambda = 2.4$ . This value of the trilinear self-coupling corresponds to a maximally destructive interference between triangle-like and box-like diagrams. For  $\kappa_\lambda = 1$ , the maximal destructive interference happens at the  $HH$  production threshold and therefore does not manifest itself as a dip, while for  $\kappa_\lambda$  values larger than  $\sim 3$  the triangle-type contributions start to dominate.

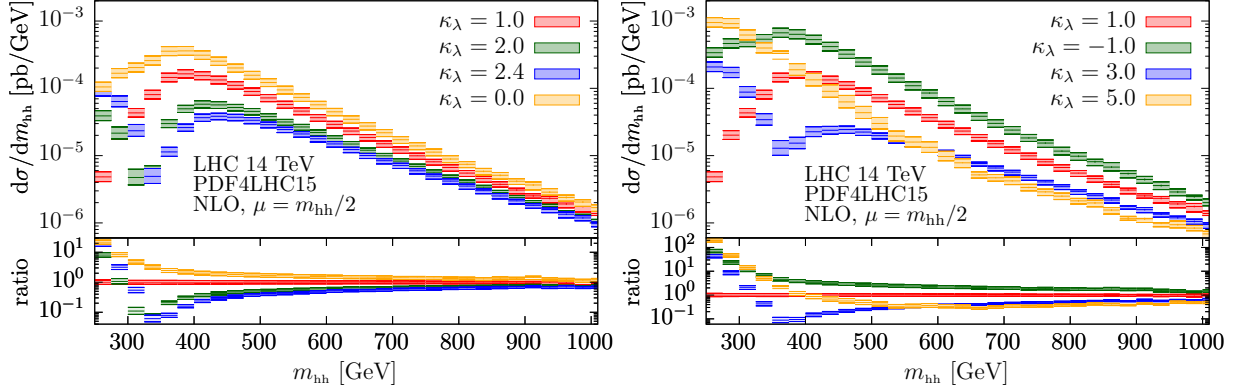


**Figure 3.** Distributions of the Higgs boson pair invariant mass  $m_{hh}$  for various values of  $\kappa_\lambda$  at  $\sqrt{s} = 14$  TeV. The uncertainty bands are from scale variations as described in the text.

Note that since the contributions can be separated in triangle- and box-like diagrams, the top-Higgs Yukawa coupling  $y_t$  can easily be varied within the same code. A non-SM value of  $y_t$  yields in Eq. (1):

$$|\mathcal{M}_\lambda|^2 = y_t^4 \left[ \mathcal{M}_B^* \mathcal{M}_B + \frac{\kappa_\lambda}{y_t} (\mathcal{M}_B^* \mathcal{M}_T + \mathcal{M}_T^* \mathcal{M}_B) + \left( \frac{\kappa_\lambda}{y_t} \right)^2 \mathcal{M}_T^* \mathcal{M}_T \right]. \quad (3)$$

The cross-section can be computed by setting the correct value of the ratio  $\kappa_\lambda/y_t$  and of the global rescaling factor. For example,  $\sigma(y_t = 1.2, \kappa_\lambda = 1) = (1.2)^4 \sigma(y_t = 1, \kappa_\lambda = 1/1.2)$ . Fig. 4 shows the distribution of  $m_{hh}$  for values of the top-Higgs Yukawa coupling that are still not experimentally excluded [4].

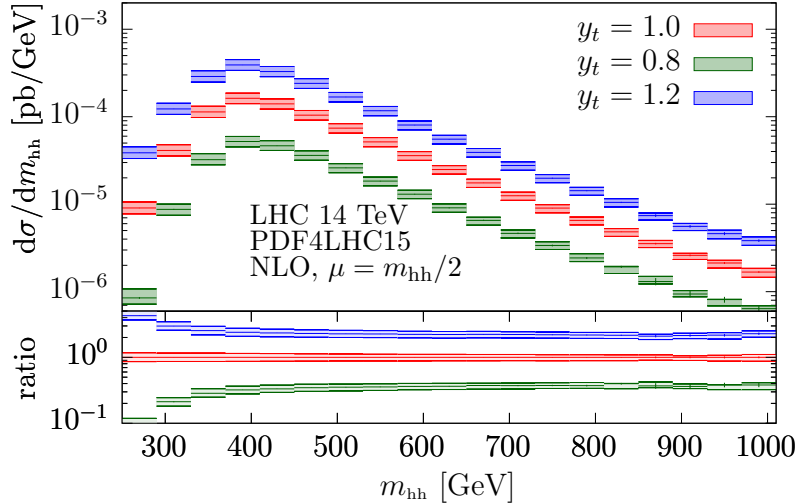


**Figure 4.** The distribution of the Higgs boson pair invariant mass  $m_{hh}$  for values of the top-Higgs Yukawa coupling  $y_t \in \{0.8, 1, 1.2\}$ .

#### 4. Parton-shower matched results

We now consider NLO distributions matched to a parton shower. The Les Houches Events (LHE) [45] files produced by `Powheg` are used as input to the `Pythia8.235` and `Herwig7.1.4`

parton showers. In the case of **Herwig7**, both the default angular-ordered  $\tilde{q}$  and the dipole showers are compared. The radiation-regulating **hdamp** parameter in **Powheg** is set to **hdamp** = 250 GeV. Multiple-parton interactions and hadronisation are switched off. The default tunes are used for both parton showers.

Fig. 5 displays the transverse momentum of the Higgs boson pair  $p_T^{hh}$  and the separation between the two Higgs bosons  $\Delta R^{hh} = \sqrt{(\eta_1 - \eta_2)^2 + (\phi_1 - \phi_2)^2}$ . Considering first the distribution of  $p_T^{hh}$ , both **Herwig7** parton showers (PH7- $\tilde{q}$  and PH7-dipole) generate similar results and reproduce the fixed-order NLO prediction in the far- $p_T^{hh}$  range. In contrast, **Pythia8** agrees with **Herwig7** only for small transverse momenta, while it produces much harder radiation in the tail of the distribution. The same comments apply to the  $\Delta R^{hh}$  observable in the region  $0 < \Delta R^{hh} < \pi$  where shower contributions are important. Large parton-shower matching uncertainties in Higgs boson pair production have already been discussed in Ref. [46].

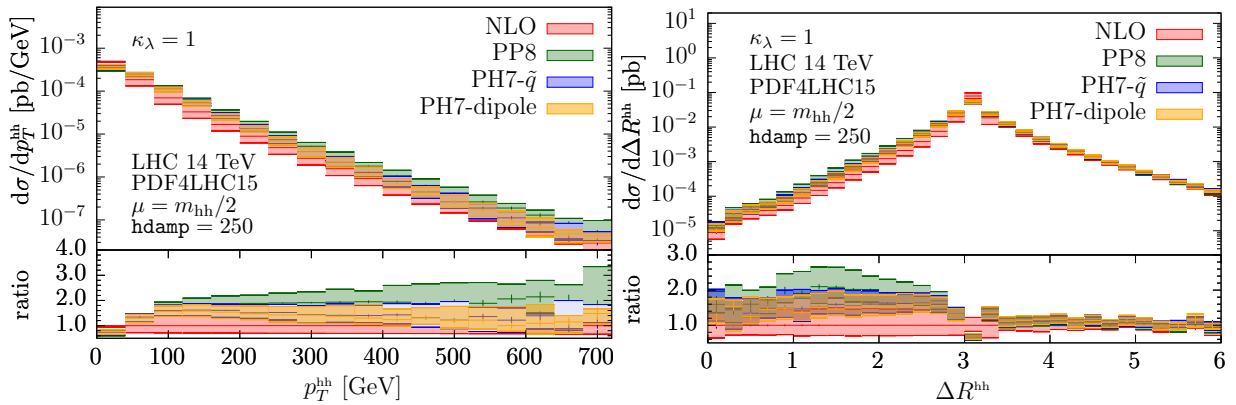


**Figure 5.** The transverse momentum  $p_T^{hh}$  of the Higgs boson pair and the separation between the two Higgs bosons  $\Delta R^{hh}$  are shown for the fixed-order NLO calculation and three parton showers, in the  $\kappa_\lambda = 1$  case.

## 5. Conclusion

We have presented a new program package for Higgs boson pair production at NLO QCD with full top-quark mass dependence. In this package, the trilinear Higgs self-coupling can be varied explicitly. Within the same code, simultaneous variations of the top-Higgs Yukawa coupling can also be produced. The public code for the **Powheg-BOX-V2** event generator can be found at the website <http://powhegbox.mib.infn.it> in the **User-Processes-V2/ggHH** subdirectory. In addition, approximations related to the heavy top limit (HTL) can be enabled for comparison purposes. We have found that the full  $m_t$ -dependent NLO QCD corrections lead to  $K$ -factors which exhibit a sizeable dependence on the value of the trilinear Higgs self-coupling, which is not present in the HTL. We have compared fixed-order predictions at NLO QCD to parton-shower matched results. Both the **Pythia8** and **Herwig7** ( $\tilde{q}$  and dipole) parton showers can be matched directly to LHE files produced by **Powheg**. Full particle-level events can be produced with our framework, including Higgs boson decays and hadronisation.

## References

- [1] Aad G *et al.* (ATLAS, CMS) 2016 *JHEP* **08** 045 (*Preprint* 1606.02266)
- [2] Aaboud M *et al.* (ATLAS) 2018 *JHEP* **03** 095 (*Preprint* 1712.02304)
- [3] Sirunyan A M *et al.* (CMS) 2018 *Submitted to: Eur. Phys. J.* (*Preprint* 1809.10733)
- [4] Sirunyan A M *et al.* (CMS) 2018 *Submitted to: Phys. Lett.* (*Preprint* 1812.06504)
- [5] Sirunyan A M *et al.* (CMS) 2019 *Phys. Rev. Lett.* **122** 121803 (*Preprint* 1811.09689)

- [6] ATLAS 2018 Combination of searches for Higgs boson pairs in  $pp$  collisions at 13 TeV with the ATLAS experiment. Tech. Rep. ATLAS-CONF-2018-043 CERN Geneva URL <https://cds.cern.ch/record/2638212>
- [7] Dawson S, Dittmaier S and Spira M 1998 *Phys. Rev.* **D58** 115012 (*Preprint hep-ph/9805244*)
- [8] de Florian D and Mazzitelli J 2013 *Phys. Rev. Lett.* **111** 201801 (*Preprint 1309.6594*)
- [9] Grigo J, Melnikov K and Steinhauser M 2014 *Nucl. Phys.* **B888** 17–29 (*Preprint 1408.2422*)
- [10] de Florian D, Grazzini M, Hanga C, Kallweit S, Lindert J M, Maierhöfer P, Mazzitelli J and Rathlev D 2016 *JHEP* **09** 151 (*Preprint 1606.09519*)
- [11] Borowka S, Greiner N, Heinrich G, Jones S, Kerner M, Schlenk J, Schubert U and Zirke T 2016 *Phys. Rev. Lett.* **117** 012001 [Erratum: *Phys. Rev. Lett.* 117, no. 7, 079901 (2016)] (*Preprint 1604.06447*)
- [12] Borowka S, Greiner N, Heinrich G, Jones S, Kerner M, Schlenk J and Zirke T 2016 *JHEP* **10** 107 (*Preprint 1608.04798*)
- [13] Baglio J, Campanario F, Glaus S, Mühlleitner M, Spira M and Streicher J 2018 (*Preprint 1811.05692*)
- [14] Buchalla G, Capozzi M, Celis A, Heinrich G and Scyboz L 2018 *JHEP* **09** 057 (*Preprint 1806.05162*)
- [15] Nason P 2004 *JHEP* **11** 040 (*Preprint hep-ph/0409146*)
- [16] Frixione S, Nason P and Oleari C 2007 *JHEP* **11** 070 (*Preprint 0709.2092*)
- [17] Alioli S, Nason P, Oleari C and Re E 2010 *JHEP* **06** 043 (*Preprint 1002.2581*)
- [18] Sjostrand T, Ask S, Christiansen J R, Corke R, Desai N, Ilten P, Mrenna S, Prestel S, Rasmussen C O and Skands P Z 2015 *Comput. Phys. Commun.* **191** 159–177 (*Preprint 1410.3012*)
- [19] Bellm J *et al.* 2017 (*Preprint 1705.06919*)
- [20] Heinrich G, Jones S P, Kerner M, Luisoni G and Scyboz L 2019 (*Preprint 1903.08137*)
- [21] Heinrich G, Jones S P, Kerner M, Luisoni G and Vryonidou E 2017 *JHEP* **08** 088 (*Preprint 1703.09252*)
- [22] Luisoni G, Nason P, Oleari C and Tramontano F 2013 *JHEP* **10** 083 (*Preprint 1306.2542*)
- [23] Cullen G, Greiner N, Heinrich G, Luisoni G, Mastrolia P, Ossola G, Reiter T and Tramontano F 2012 *Eur. Phys. J.* **C72** 1889 (*Preprint 1111.2034*)
- [24] Cullen G *et al.* 2014 *Eur. Phys. J.* **C74** 3001 (*Preprint 1404.7096*)
- [25] Peraro T 2014 *Comput. Phys. Commun.* **185** 2771–2797 (*Preprint 1403.1229*)
- [26] Binoth T, Guillet J P, Heinrich G, Pilon E and Reiter T 2009 *Comput. Phys. Commun.* **180** 2317–2330 (*Preprint 0810.0992*)
- [27] Cullen G, Guillet J P, Heinrich G, Kleinschmidt T, Pilon E *et al.* 2011 *Comput. Phys. Commun.* **182** 2276–2284 (*Preprint 1101.5595*)
- [28] van Hameren A 2011 *Comput. Phys. Commun.* **182** 2427–2438 (*Preprint 1007.4716*)
- [29] Arnold K *et al.* 2009 *Comput. Phys. Commun.* **180** 1661–1670 (*Preprint 0811.4559*)
- [30] Baglio J *et al.* 2014 (*Preprint 1404.3940*)
- [31] Jones S P 2016 *PoS LL2016* 069 (*Preprint 1608.03846*)
- [32] von Manteuffel A and Studerus C 2012 (*Preprint 1201.4330*)
- [33] Borowka S, Heinrich G, Jones S P, Kerner M, Schlenk J and Zirke T 2015 *Comput. Phys. Commun.* **196** 470–491 (*Preprint 1502.06595*)
- [34] Borowka S, Heinrich G, Jahn S, Jones S P, Kerner M and Schlenk J 2018 *Comp. Phys. Comm.* (*Preprint 1811.11720*)
- [35] Jones S P 2019 *These Proceedings*
- [36] Butterworth J *et al.* 2015 (*Preprint 1510.03865*)
- [37] Dulat S, Hou T J, Gao J, Guzzi M, Huston J, Nadolsky P, Pumplin J, Schmidt C, Stump D and Yuan C P 2016 *Phys. Rev.* **D93** 033006 (*Preprint 1506.07443*)
- [38] Harland-Lang L A, Martin A D, Motylinski P and Thorne R S 2015 *Eur. Phys. J.* **C75** 204 (*Preprint 1412.3989*)
- [39] Ball R D *et al.* (NNPDF) 2015 *JHEP* **04** 040 (*Preprint 1410.8849*)
- [40] Buckley A, Ferrando J, Lloyd S, Nordström K, Page B, Rüfenacht M, Schönherr M and Watt G 2015 *Eur. Phys. J.* **C75** 132 (*Preprint 1412.7420*)
- [41] Cacciari M, Salam G P and Soyez G 2008 *JHEP* **04** 063 (*Preprint 0802.1189*)
- [42] Cacciari M and Salam G P 2006 *Phys. Lett.* **B641** 57–61 (*Preprint hep-ph/0512210*)
- [43] Cacciari M, Salam G P and Soyez G 2012 *Eur. Phys. J.* **C72** 1896 (*Preprint 1111.6097*)
- [44] Gröber R, Mühlleitner M, Spira M and Streicher J 2015 *JHEP* **09** 092 (*Preprint 1504.06577*)
- [45] Alwall J *et al.* 2007 *Comput. Phys. Commun.* **176** 300–304 (*Preprint hep-ph/0609017*)
- [46] Jones S and Kuttimalai S 2018 *JHEP* **02** 176 (*Preprint 1711.03319*)